

Additive Effect of Kirkendall Void Formation in Sn-3.5Ag Solder Joints on Common Substrates

FENG GAO,^{1,3} HIROSHI NISHIKAWA,¹ and TADASHI TAKEMOTO¹

1.—Joining and Welding Research Institute, Osaka University, 11-1 Mihogaoka, Ibaraki-shi, Osaka 567-0047, Japan. 3.—e-mail: gaofj@jwri.osaka-u.ac.jp

The Sn-3.5Ag and Sn-3.5Ag-0.2Co-0.1Ni lead-free solders were investigated on common electronics substrates, namely, organic solderability preservative (OSP) and electroless Ni/immersion Au (ENIG) surface finishes. The formation of Kirkendall voids at the interfacial region during isothermal solid aging was explored. For the Sn-3.5Ag-0.2Co-0.1Ni/OSP solder joint, the Kirkendall voids were present after isothermal solid-state aging at higher temperature (e.g., 150°C); however, the size of voids did not change remarkably with prolonged aging time due to the depressed Cu₃Sn layer growth. For ENIG surface finishes, the 0.2Co-0.1Ni additions seemed to enhance the longitudinal groove-shaped voids at the Ni₃P layer; however, void formation at the solder/Ni₃Sn₄ interface was effectively reduced. This might be attributed to the reduced Sn activity in the solder matrix and the suppressed Ni-P-Sn layer formation.

Key words: Lead-free solder, Sn-3.5Ag, additive, Kirkendall void, diffusion, thermodynamics

INTRODUCTION

With the trend toward miniaturization in consumer electronics, the size of electronic components and thus solder joints is being continuously scaled down. Moreover, it has been demonstrated that electromigration has a remarkable effect on the initiation and propagation of Kirkendall voids.^{1,2} Therefore, Kirkendall voids have emerged as a serious reliability threat for solder joint, and this research topic has been developed into a critical area of interest. It has been reported previously that extensive Kirkendall voids are generated at the solder/Cu interface and deteriorate the reliability of the solder joint under impact or shock loads.³⁻⁴ Usually, the voids were generated and coalesced at the Cu/Cu₃Sn interface or within the Cu₃Sn phase layer for the OSP/Cu substrate, while they were located at the P-rich layer or P-rich/Sn-Ni intermetallic interface for electroless Au/Ni ENIG substrate. Mei et al. have reported several cases of Kirkendall void in electronic packaging. In partic-

ular, they found that the presence of Ni in either the Cu substrate or the solder joint might reduce the void density.⁵ The Bi species in Sn-Bi lead-free solder can segregate into the Cu/Cu₃Sn interface and take up the vacancy sink, thereby causing vacancy condensation and greater void formation.⁶ Recently, it was found that Cu substrate with larger than 5 wt.% Ni could prevent the formation of the (Cu,Ni)₃Sn layer during isothermal aging, and thus influence the formation of Kirkendall voids, although the growth of (Cu,Ni)₆Sn₅ intermetallic was in turn significantly promoted.⁷

Two approaches are feasible to depress the formation of microvoids at solder joints, that is, the development of new printed circuit board (PCB) surface finishes or the new lead-free solders. So far, the OSP and ENIG surface finishes are the most common substrates utilized in electronic assembly. The ENIG finish is attractive due to its simplicity and the low cost of the manufacturing process, and also acts as an effective barrier for interfacial reactions. OSP is also a widely used surface finish, and is especially used to avoid “black pad” failures. Thus developing new solders by alloying Sn-Ag or Sn-Ag-Cu solder candidates seems convenient and applicable. The present authors have found that Co-Ni dual addition into the

(Received March 8, 2007; accepted July 31, 2007; published online September 21, 2007)

Sn-3.5Ag binary eutectic solder alloy can depress the formation of Cu_3Sn at the solder/Cu interface, which implies that the interdiffusion of Sn/Cu is altered, in particular at the isothermal aging temperature. Therefore using this alloying methodology, the Kirkendall voiding behavior between the Sn-3.5Ag-based solder alloys and common substrates (*i.e.*, OSP and ENIG) was explored in this paper.

EXPERIMENTAL PROCEDURES

Two sorts of lead-free solder alloys, Sn-3.5Ag and Sn-3.5Ag-0.2Co-0.1Ni (Nihon Genma Co. Ltd., hereafter, simply referred as SA and SA-CoNi, respectively) were soldered on OSP and ENIG substrates, respectively. The diameter of the surface finish pads was $800\ \mu\text{m}$. The thickness of the Cu pad was $35\ \mu\text{m}$, and there was a $5\ \mu\text{m}$ Ni(P)/Au finish on the Cu layer for the ENIG substrate. All the surface finishes were chemically treated in 4% HCl solution and then cleaned ultrasonically in ethanol. Commercial rosin mildly activated (RMA) flux was applied during soldering, which was performed at 250°C for 1 min under a controlled nitrogen atmosphere. Some of the solder joints were subjected to the isothermal aging at 150°C for 504 and 1008 h, respectively. The microstructure was observed by scanning electron microscopy (SEM, JSM-6320F, JEOL Co. LTD., Japan), and the chemical composition was measured by electron probe microanalysis (EPMA) from JEOL Co. LTD., Japan.

RESULTS AND DISCUSSION

Interfacial Reaction on OSP Finish

The microstructure comparison of the solder alloys on OSP finish is illustrated in Fig. 1. Apparently, a Cu_6Sn_5 intermetallic layer with $1.5\ \mu\text{m}$ thickness was formed at the SA/OSP interface after reflow, and a large size of Ag_3Sn plate is also observed at the interface and also penetrating into the solder matrix. For the SA-CoNi/OSP solder joint, the $(\text{Cu},\text{Co},\text{Ni})_6\text{Sn}_5$ intermetallic is formed and the thickness is about $5.2\ \mu\text{m}$. The Co and Ni solubilities were 5.4 and 5.1 at.%, respectively. Some of the $(\text{Co}_{0.9},\text{Ni}_{0.1})\text{Sn}_2$ intermetallics are located near the solder/OSP interface. There are some voids in the $(\text{Cu},\text{Co},\text{Ni})_6\text{Sn}_5$ phase, which might be attributed to the solder entrapped in the nondense and refined intermetallic structure.⁸ After isothermal aging at 150°C for 504 h, the Co and Ni solubilities in the $(\text{Cu},\text{Co},\text{Ni})_6\text{Sn}_5$ phase were reduced to 3.7 and 1.7 at.%, respectively. In addition, the Cu_3Sn phase layer in the SA-CoNi/OSP solder joint is only $1.2\ \mu\text{m}$ in thickness, which is substantially thin than that of the SA/OSP solder joint, namely, $3.0\ \mu\text{m}$. Kirkendall voids were observed at both solder joints, mainly located within the Cu_3Sn phase or at the $\text{Cu}_3\text{Sn}/\text{Cu}$ interface. The average sizes of voids at the solder joints are about 0.50 and $0.35\ \mu\text{m}$ for SA/OSP and SA-CoNi/OSP,

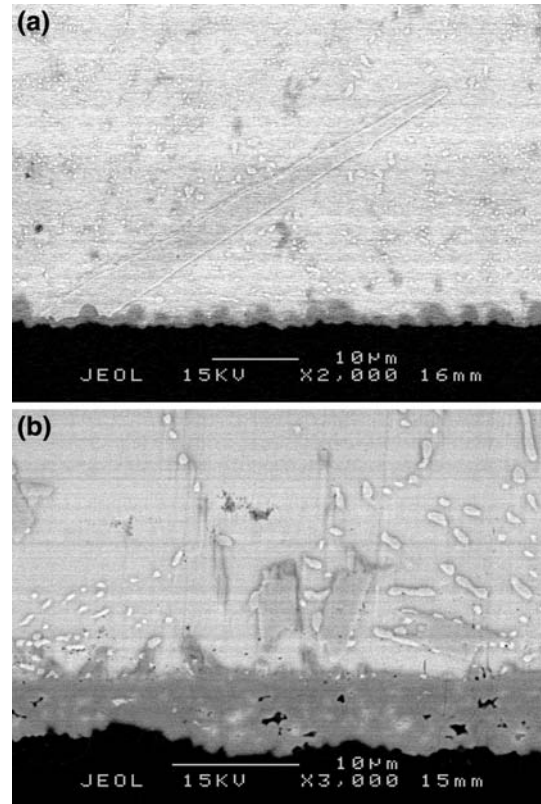


Fig. 1. Interfacial reaction of SA and SA-CoNi solder alloys on OSP finish at 250°C for 1 min: (a) SA/OSP and (b) SA-CoNi/OSP.

respectively. The voids were not uniformly distributed at the Cu_3Sn or near the $\text{Cu}_3\text{Sn}/\text{Cu}$ interface, and the void density for SA-CoNi/OSP was slightly greater.

After the prolonged isothermal aging for 1008 h the evolution of the Kirkendall voids is illustrated in Fig. 3. For the SA-CoNi/OSP solder joint, the thickness of the Cu_3Sn phase layer is still quite small, say, $1.3\ \mu\text{m}$, and there is no visible change of the void size. However, for the SA/OSP solder joint, the Cu_3Sn intermetallic continues to grow up to $3.8\ \mu\text{m}$ in thickness. The Kirkendall voids are also growing, and the diameter of some voids becomes as large as $1\ \mu\text{m}$. Therefore, the addition of Co-Ni to Sn-3.5Ag solder is effective to depress the growth of Kirkendall voids, in particular under long isothermal aging.

As we know, in the diffusion processes, the formation of void is due to the unbalanced diffusion flux of one species compared to the opposite flux of another species. Voids have been reported in several works, including Kirkendall voids. The rapid diffusion of one material into another can cause crystal vacancies to form in the bulk material. These vacancies attract each other, which results in the formation of so-called Kirkendall voids. It has been demonstrated that at an isothermal aging temperature of, e.g., 150°C , Cu atoms are the dominant

diffusion species in Cu_6Sn_5 intermetallic.⁹ In addition, since the unit cell of the Cu_3Sn phase has three Cu atoms and one Sn atoms, the lattice sites of Cu form a continuous chain for substitutional diffusion of Cu. The substitutional diffusion of Sn will take antisite jumps, and thus it is reasonable to expect that Cu is also the dominant diffusion species in Cu_3Sn .³ Apparently, the interdiffusion flux difference between Sn and Cu atoms is still present for both SA/OSP and SA-CoNi/OSP solder joints. Due to the unequal intrinsic diffusion flux of Cu and Sn at the Cu_3Sn /OSP interface, the atomic-level vacancies left by the migrating Cu atoms on the bare Cu substrate are not filled by Sn atoms, and these vacancies coalesce into Kirkendall voids. Obviously, Cu atoms will diffuse faster along the Cu_6Sn_5 grain boundaries. For the SA/OSP solder joint, the voids will continue to grow due to the continuous formation of Cu_3Sn . However, the grain size of the $(\text{Cu},\text{Co},\text{Ni})_6\text{Sn}_5$ intermetallic at the SA-CoNi/OSP solder joint is greatly refined owing to the Co-Ni solubility.⁸ Thus the void density might be slight enhanced because of the possible provision of Cu diffusion channels. Due to the suppressed reaction of Cu_3Sn formation, the growth of the voids for the SA-CoNi/OSP solder joint is also depressed and therefore the size of void does not increase with aging time.

Another interesting phenomenon is the distribution of the Kirkendall voids, which can serve as diffusion markers. For the SA-CoNi/OSP solder joint, the voids are mainly located near the Cu_3Sn /OSP interface, while more than half amount of the voids are within the Cu_3Sn layer at the SA/OSP solder joint. Zeng et al. reported that the growth of Cu_3Sn can take place either by reacting three Cu atoms with one Sn atom or by the decomposition of Cu_6Sn_5 . When one formula of Cu_6Sn_5 is converted into Cu_3Sn , it releases three Sn atoms³



While the majority of the released Sn atoms will react with the incoming Cu atoms at the $\text{Cu}_6\text{Sn}_5/\text{Cu}_3\text{Sn}$ interface, some of the Sn atoms may diffuse to the $\text{Cu}_3\text{Sn}/\text{Cu}$ interface and react with the Cu pad there, resulting in the growth of the Cu_3Sn layer towards the OSP substrate. Apparently, the existing voids at the $\text{Cu}_3\text{Sn}/\text{Cu}$ interface will remain there if Cu is the only diffusing species. On the other hand, the void will be displaced into the Cu_3Sn when some the Sn atoms diffuse to the $\text{Cu}_3\text{Sn}/\text{OSP}$ interface to react with the Cu behind the void. For the SA/OSP solder joint, almost half of the voids are located within the Cu_3Sn layer, which implies that some of Sn atoms diffuse across the Cu_3Sn and react with the Cu atoms there. The growth of Cu_3Sn is at the expense of Cu_6Sn_5 . However, for SA-CoNi/OSP, the majority of the voids are near the $\text{Cu}_3\text{Sn}/\text{Cu}$ interface. The movement trace of the voids indicates that the decomposition of the

Cu_6Sn_5 phase at the SA/OSP joint is more severe than that of SA-CoNi/OSP joint.

It has been found by the present authors that the presence of (Co, Ni) solubility in the $(\text{Cu},\text{Co},\text{Ni})_6\text{Sn}_5$ phase at the SA-CoNi/OSP solder joint can stabilize the Cu_6Sn_5 phase,⁸ which indicates that the decomposition of Cu_6Sn_5 phase will be substantially reduced. Fewer Sn atoms will be released and fewer Sn atoms can diffuse across the Cu_3Sn phase to react with Cu atoms. Therefore, Kirkendall voids will mostly be located near the $\text{Cu}_3\text{Sn}/\text{OSP}$ interface, which is quite consistent with the observations. In addition, compared with SA-CoNi/OSP, the Cu_6Sn_5 layer of SA/OSP is much thinner due to its decomposition, as illustrated in Figs. 2 and 3.

Interfacial Reaction on ENIG Finish

Figure 4 shows the microstructure of the as-reflowed solder joints on the ENIG substrate. For both SA/ENIG and SA-CoNi/ENIG solder joints, faceted interfacial reactive products are generated. The intermetallic phases at the interface for both cases are identified as Ni_3Sn_4 based on EPMA. Only a very small amount of Co solubility (~ 1.0 at.%) is detected in Ni_3Sn_4 at the SA-CoNi/ENIG solder joint. This may be attributed to the interaction difference between the Ni/Sn and Co/Sn couples. Since the Ni/Sn couple possesses a higher affinity

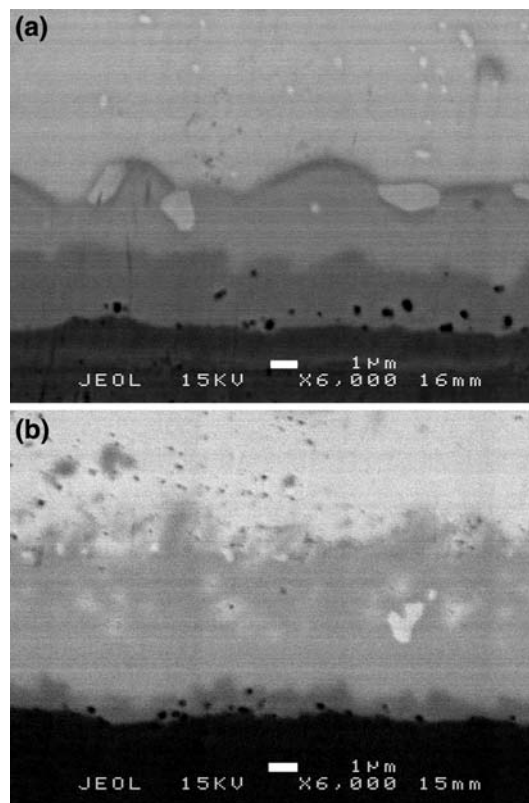


Fig. 2. Solder/OSP joints after aging at 150°C for 504 h: (a) SA/OSP and (b) SA-CoNi/OSP.

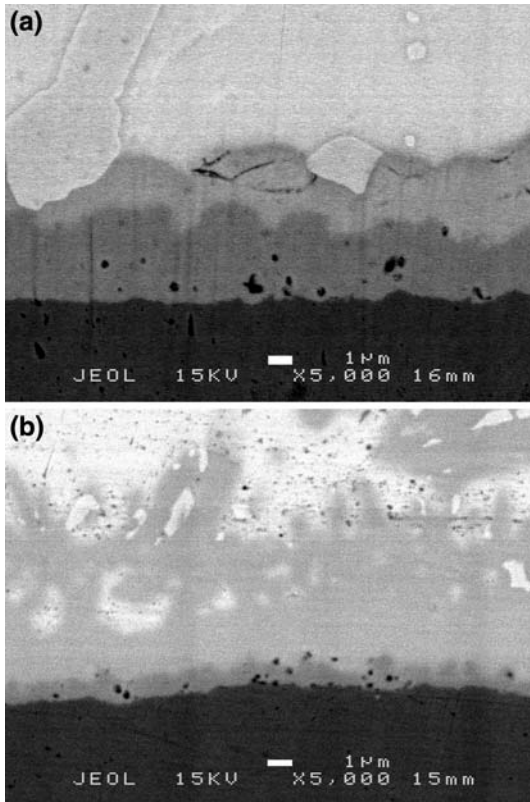


Fig. 3. Solder/OSP joints after aging at 150°C for 1,008 h: (a) SA/OSP (b) and SA-CoNi/OSP.

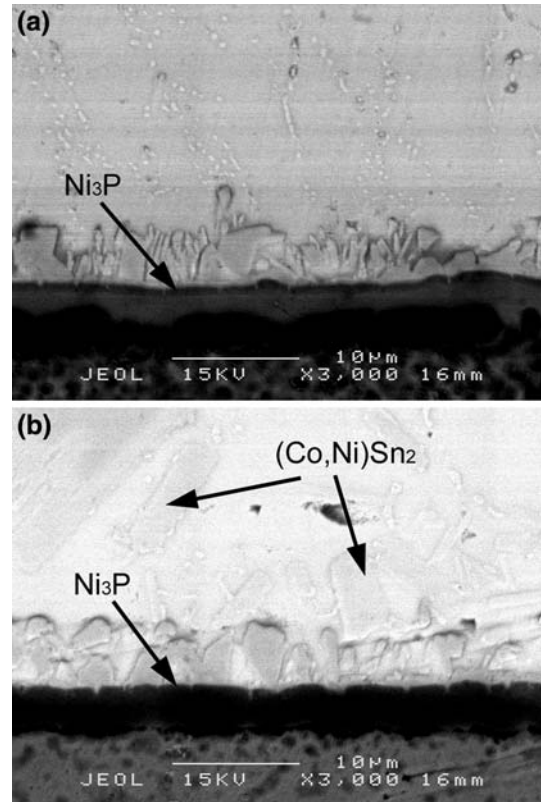


Fig. 4. Interfacial reaction of SA and SA-CoNi solder alloys on ENIG substrate at 250°C for 1 min: (a) SA/ENIG and (b) SA-CoNi/ENIG.

than the Co/Sn couple, the participation of Co atoms to replace Ni lattice sites in Ni_3Sn_4 cell tends to be quite difficult.⁸

Figure 5 shows the interfacial reaction evolution of the SA/ENIG and SA-CoNi/ENIG solder joints after isothermal aging at 150°C for 504 h. The formation of Ni_3Sn_4 depletes Ni atoms from the top side of the Ni(P) layer, resulting in the formation of P-rich (Sn-P-Ni) and Ni_3P layers.⁹ In Fig. 5b, the Sn-P-Ni layer is almost invisible at the SA-CoNi/ENIG solder joint. In addition, due to the magnification and resolution of SEM, the voids at the Sn-P-Ni layer are not so clear in the current study. Therefore, void formation in the Sn-P-Ni layer will be further studied and discussed elsewhere. The thickness of the Ni_3P layer is 0.7 and 1.0 μm for SA/ENIG and SA-CoNi/ENIG, respectively. Some of the groove-like voids are located at the Ni_3P layer and perpendicular to the Ni_3P layer. It seems that the formation of the groove-like voids at the SA-CoNi/ENIG solder joint is more severe than for SA/ENIG. There is no clear sign of voids at the $\text{Ni}_3\text{Sn}_4/\text{Ni-P-Sn}$ interface. However, some voids with a diameter of 1 to 2 μm are formed at the SA solder/ Ni_3Sn_4 interface. After prolonged isothermal aging at 150°C for 1008 h the Sn-P-Ni layer tends to be clear, which can be identified based on the contrast difference from Ni_3Sn_4 and Ni_3P , as shown in

Fig. 6a and b. The thickness of Sn-P-Ni and Ni_3P is 0.4 and 0.8 μm for the SA/ENIG joint, and 0.1 and 1.0 μm for the SA-CoNi/ENIG solder joint, respectively. Moreover, a small amount of Co, 1.4 at.%, is detected in the Sn-P-Ni layer at the SA-CoNi/ENIG solder joint. The size and amount of the groove-like voids in the Ni_3P layer both increase for both solder joints with the aging time. It has been reported that these longitudinal groove-like voids do not have an impact on shock or drop test performance.¹⁰ However, no visible voids are formed at the $\text{Ni}_3\text{Sn}_4/\text{Ni-P-Sn}$ interface. For the SA/ENIG solder joint, the voids located at the solder/ Ni_3Sn_4 interface tend to be worse, while no such voids are found at the SA-CoNi/ Ni_3Sn_4 interface, as shown in Fig. 6a and b.

Kirkendall voids are formed at the solder/ Ni_3Sn_4 interface because the Sn atom has a faster diffusion rate compared to both Ni and P.¹¹ Due to the presence of Ni_3P layer between the Ni_3Sn_4 and ENIG, further supply of Ni atoms to the Ni_3Sn_4 IMCs requires diffusion of Ni atoms from the unreacted Ni(P) layer through the Ni_3P layer. The diffusion of Ni atoms through the Ni_3P layer is much easier than the diffusion of Sn atoms through the Ni_3P layer. This unbalanced elemental diffusion results in the growth of both the Ni_3P layer and the Kirkendall voids inside the Ni_3P layer.^{12–13} Similarly, the voids formed at the solder/ Ni_3Sn_4 are due

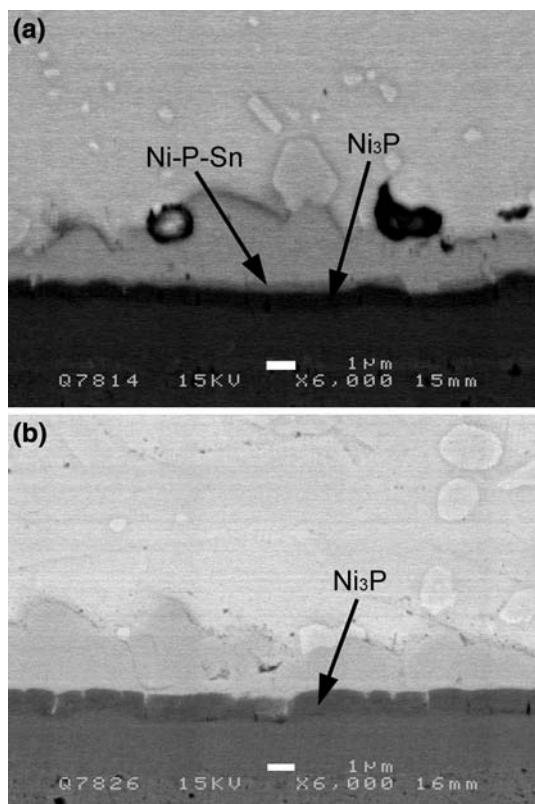


Fig. 5. Solder/ENIG joints after aging at 150°C for 504 h: (a) SA/ENIG and (b) SA-CoNi/ENIG.

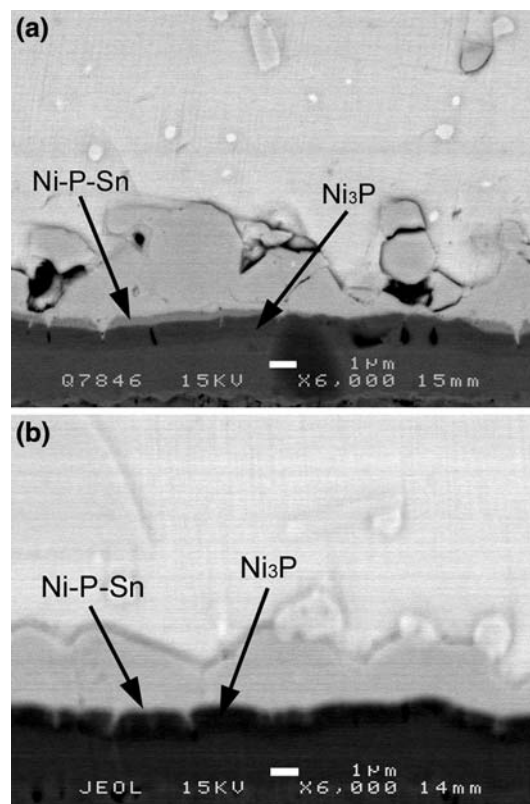


Fig. 6. Solder/ENIG joints after aging at 150°C for 1008 h: (a) SA/ENIG and (b) SA-CoNi/ENIG.

to the unbalanced diffusive flux of Sn from the solder matrix and the Ni atoms from Ni_3P or Ni(P).

The addition of Co-Ni to the Sn-3.5Ag eutectic solder enhances the groove-like voids in the Ni_3P layer. However, the voids at the solder/ Ni_3Sn_4 interface are remarkably reduced for the SA-CoNi/ENIG solder joint. The reason behind these phenomena is explored herein. Although the solubility of Co and Ni in Sn is quite small, based on the EPMA measurements, a small amount of Co (~ 0.15 at.%) and Ni (~ 0.04 at.%) can still be detected in the β -Sn phase. Thus thermodynamics may be utilized to estimate the interaction of the component elements. The detail of the thermodynamic model can be found in Ref. 8. Figure 7 illustrates the interaction behavior of the elements in the SA-CoNi solder matrix. Obviously, the Sn atoms show a high affinity for the Co and Ni additives, while the Ag atoms exhibit very weak affinity with the additives. The voids at the solder/ Ni_3Sn_4 interface are attributed to the faster Sn diffusive flux than the opposite Ni diffusive flux from the substrate. Since the Co and Ni have a higher affinity with Sn atoms, the activity of the Sn atoms in the solder matrix is depressed according to the thermodynamic theory.¹⁴ Thus it can be reasoned that the diffusion rate of Sn through the Ni_3Sn_4 layer will be slowed down and reduce the difference from the interdiffusion flux from Ni. Another interesting phenomenon is that the Ni-P-Sn

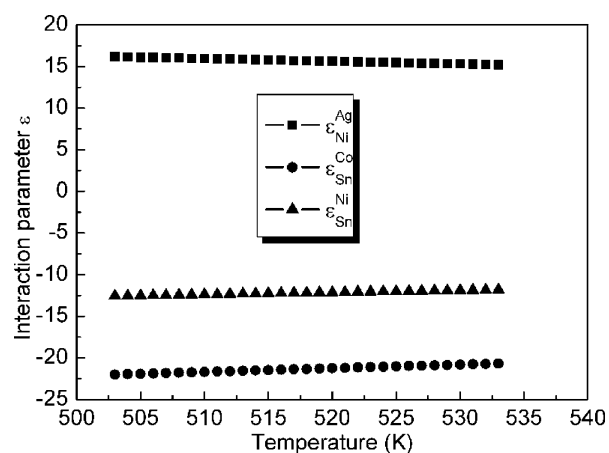


Fig. 7. The interaction behavior of the component elements in the SA-CoNi solder matrix.

layer is much thinner at the SA-CoNi/ENIG joint than at the SA/ENIG joint. This indicates that, for SA-CoNi/ENIG, the Ni diffusion flux from Ni_3P or Ni(P) will be less consumed by the formation of the Ni-P-Sn layer, thereby further reducing the unequal interdiffusion between Sn and Ni at the solder/ Ni_3Sn_4 interface. As a result, the formation of Kirkendall voids at the solder/ Ni_3Sn_4 interface is depressed in the SA-CoNi/ENIG solder joint.

In addition, the diffusion of Ni atoms through the Ni_3P layer was much easier than for Sn atoms through the Ni_3P layer. The depressed Sn activity in the SA-CoNi solder matrix will promote the unequal diffusion flux between Sn and Ni at the Ni_3P layer. Furthermore, the depressed Ni-P-Sn layer will also promote the Ni diffusion through the intermetallic layers. Therefore, the groove-like voids are slightly enhanced in the SA-CoNi/ENIG solder joint.

CONCLUSIONS

The effect of dual addition of Co-Ni on the formation of Kirkendall voids at Sn-3.5Ag/OSP and Sn-3.5Ag/ENIG solder joints were investigated. The following conclusions may be formulated:

- (a) For the interfacial reaction on the OSP substrate, Co-Ni dual addition to the Sn-3.5Ag solder alloy can significantly depress the formation of the Cu_3Sn layer during isothermal aging. The size of the Kirkendall voids at the SA-CoNi/OSP solder joint is smaller than that at the SA/OSP joint, in particular with longer isothermal aging time. The voids at the SA-CoNi/OSP solder joint are mainly located near the Cu_3Sn /OSP interface. This is attributed to the depressed decomposition of the Cu_6Sn_5 phase, since the Co-Ni solubility in Cu_6Sn_5 can stabilize this phase.
- (b) For the interfacial reaction on the ENIG substrate, groove-like voids perpendicular to the Ni_3P layer are detected at both the SA/ENIG and SA-CoNi/ENIG solder joints. It seems that these groove-like voids are enhanced to some extent by the Co-Ni addition. For the SA/ENIG joint, some amount of voids is formed at the

solder/ Ni_3Sn_4 interface, while no such voids are found at the SA-CoNi/ENIG solder joint. This might be due to the depressed Sn activity in the SA-CoNi solder matrix and the suppressed formation of Ni-P-Sn layer during the isothermal aging process at the SA-CoNi/ENIG solder joint.

ACKNOWLEDGEMENT

The authors would like to acknowledge financial support from the Japan Society for the Promotion of Science (JSPS).

REFERENCES

1. H. Gan and K.N. Tu, *J. Appl. Phys.* 97, 063514 (2005).
2. M. Ding, G.T. Wang, B. Chao, P.S. Ho, P. Su, and T. Uehling, *J. Appl. Phys.* 99, 094906 (2006).
3. K.J. Zeng, R. Stierman, T.-C. Chiu, D. Edwards, K. Ano, and K.N. Tu, *J. Appl. Phys.* 97, 024508 (2005).
4. M. Date, T. Shoji, M. Fujiyoshi, K. Sato, K.N. Tu, *Proc. Electronic Component Technology Conf.* (Las Vegas, USA, 2004), pp. 668–674.
5. Z.Q. Mei, M. Ahmad, M. Hu, G. Ramakrishna, *Proc. Electronic Component Technology Conf.* (Lake Buena Vista, USA, 2005), pp. 415–420.
6. P.L. Liu and J.K. Shang, *Scripta Mater.* 53, 631 (2005).
7. H. Yu, V. Vuorinen, J. Kivilhti, *Proc. Electronic Component Technology Conf.* (San Diego, USA, 2006), pp. 1204–1209.
8. F. Gao, T. Takemoto, H. Nishikawa, and A. Komatsu, *J. Electron. Mater.* 5, 905 (2006).
9. K.N. Tu and K. Zeng, *Mater. Sci. Eng. R.* 38, 55 (2002).
10. L.H. Xu, J.H.L. Pang, *Proc. Electronic Component Technology Conf.* (San Diego, USA, 2006), pp. 275–282.
11. P. Sun, C. Andersson, X.C. Wei, Z.N. Cheng, D.K. Shangguan, and J.H. Liu, *J. Alloys Compd.* 425, 191 (2006).
12. Z. Chen, M. He, and G. Qi, *J. Electron. Mater.* 33, 1465 (2004).
13. M. He, Z. Chen, and G. Qi, *Acta Mater.* 52, 2047 (2004).
14. X.Y. Ding, P. Fan, and W.Z. Wang, *Metall. Mater. Trans.* 30 B, 271 (1999).